

Revised version
August 2013

Anomalous Wtb coupling at the LHC

K. Kołodziej¹

*Institute of Physics, University of Silesia
ul. Uniwersytecka 4, PL-40007 Katowice, Poland*

Abstract

Some distributions of the μ^- in the top quark pair production reaction $pp \rightarrow bu\bar{d}\bar{b}\mu^-\bar{\nu}_\mu$ at the LHC are calculated to leading order in the presence of the anomalous Wtb coupling with operators of dimension up to five. The distributions in the transverse momentum, rapidity and cosine of the μ^- angle with respect to the beam in the laboratory frame and with respect to the reversed momentum of the b -quark in the rest frame of W -boson are changed rather moderately by the anomalous Wtb coupling. The distributions computed with the full set of leading order Feynman diagrams practically do not differ from those computed with the $t\bar{t}$ production diagrams, with typical acceptance cuts. This demonstrates very little effect of the off resonance background contributions.

¹E-mail: karol.kolodziej@us.edu.pl

1 Introduction.

As the top quark is very heavy, it decays even before it can hadronize, predominantly into a W -boson and a quark, with the branching fraction of $t \rightarrow Wb$ close to 1, which means that the decay at the leading order is almost exclusively governed by the Wtb coupling. Due to the almost immediate decay, the information about the top quark spin and couplings is passed to its decay products without being obscured by the hadronization process and it can be best gained from the analysis of differential cross sections, in particular from the angular distribution of the lepton from the W -boson decay [1]. Therefore the top quark production processes are ideal for tests of extensions of the standard model (SM) that lead to modifications of the pure left-handed Wtb coupling of SM. This issue has been already extensively addressed in literature, see, e.g., [2], [3], [4], [5], [6]. In [4], a decoupling theorem was proven, which states that the angular distribution of the secondary lepton resulting from a decay of the top quark produced in $e^+e^- \rightarrow t\bar{t}$ receives no contribution from the anomalous Wtb coupling in the narrow width approximation (NWA). The theorem turned out to remain correct also in a more complicated case of the off shell top quark pair production in e^+e^- annihilation and decay in 6 fermion final states including the non-double resonance background contributions, which was checked by direct computation in [6]. It was also shown [7] that the anomalous Wtb coupling cannot explain discrepancies between the forward-backward asymmetry (FBA) in the top quark pair production in high energy proton-antiproton collisions observed by the CDF [8] and D0 [9] experiments at Tevatron and the SM expectations [10]. The FBA in [7] was computed taking into account leading order cross sections of all the sub-processes of quark-antiquark annihilation, which dominate the top quark pair production at the Tevatron, of the form $q\bar{q} \rightarrow b\bar{q}'\bar{b}l\bar{\nu}_l$, with $w\bar{u}$ and $d\bar{d}$ in the initial state and a single charged lepton in the final state. In spite of the fact that off resonance contributions to such reactions are changed in the presence of the anomalous Wtb coupling, as it substantially alters the total top quark decay width, the rapidity distributions of the final state lepton remain almost unchanged. This can be considered as another example of the decoupling theorem of [4] that remains valid in the off shell top quark pair production and decay in quark-antiquark annihilation.

In the proton-proton collisions at the LHC, the top quarks are produced dominantly in pairs through the underlying gluon-gluon fusion or the quark-

antiquark annihilation processes

$$gg \rightarrow t\bar{t}, \quad q\bar{q} \rightarrow t\bar{t}. \quad (1)$$

The single top production processes, as, e.g., $qb \rightarrow q't$, $q\bar{q}' \rightarrow t\bar{b}$, or $qg \rightarrow q't\bar{b}$, have much smaller cross sections. Each of the top quarks of (1) decays into a b -quark and a W -boson, and the W -bosons decay into a fermion-antifermion pair each which leads to reactions with 6 fermions in the final state. The top quark pair production events are best identified if one of the W bosons decays leptonically and the other hadronically that corresponds to reactions of the form

$$pp \rightarrow bq\bar{q}' \bar{b}l\bar{\nu}_l. \quad (2)$$

This means that one should select events with an isolated electron or muon with large transverse momentum, a missing transverse momentum from the undetected neutrino and four or more jets.

For the sake of clarity, in the present work, we will concentrate on one specific channel of (2):

$$pp \rightarrow bu\bar{d} \bar{b}\mu^- \bar{\nu}_\mu \quad (3)$$

and address the question to which extent the anomalous Wtb coupling affects different distributions of the final state μ^- . In other words, we would like to check if the decoupling theorem of [4] holds also for the top quark pair production in proton-proton collisions at the LHC. We will also illustrate the role of the off-resonance background contributions in (3) by comparing the distributions computed with the full set of leading order Feynman diagrams with those computed with the $t\bar{t}$ production diagrams only.

2 An anomalous Wtb coupling at the LHC

The underlying hard scattering processes of (3) that contribute most to its cross section are the following:

$$gg \rightarrow bu\bar{d} \bar{b}\mu^- \bar{\nu}_\mu, \quad (4)$$

$$u\bar{u} \rightarrow bu\bar{d} \bar{b}\mu^- \bar{\nu}_\mu, \quad (5)$$

$$d\bar{d} \rightarrow bu\bar{d} \bar{b}\mu^- \bar{\nu}_\mu. \quad (6)$$

In the leading order, neglecting light fermion masses, $m_u = m_d = m_\mu = 0$, and the Cabibbo-Kobayashi-Maskawa mixing between quarks, there are 421 Feynman diagrams of the gluon-gluon fusion process (4) and 718 diagrams of each of the quark-antiquark annihilation processes (5) and (6). Some examples of the diagrams of processes (4) and (5) are shown in Figs. 1 and 2. There are 3 double resonance $t\bar{t}$ production signal diagrams of the gluon-gluon fusion processes (4): two of them are depicted in Figs. 1a and 1b and the third is obtained by interchanging the gluon lines in Fig. 1b. At the same time the quark-antiquark annihilation process (5) receives contributions from 6 $t\bar{t}$ production signal diagrams: 3 of them are depicted in Figs. 2a and 2b and the other 3 are obtained by interchanging the u -quark lines in each diagram of Figs. 2a and 2b. The Feynman diagrams of process (6) are obtained from those of process (5) just by replacing the initial state u -quarks with d -quarks. Note that if the top quarks were assumed to be produced on-shell, which corresponds to the NWA for the top quarks, then the number of the signal diagrams for each of the processes (4), (5) and (6) would be equal 3. Thus, in the NWA, not only does one neglect a plethora of background contributions represented by the diagrams in Figs. 1e, 1f and 2d, but also part of the double resonance signal diagrams and the diagrams with two or one top quark propagators, as those depicted in Figs. 1c, 1d and 2c. Let us note that the Wtb coupling that is indicated by a blob enters twice both in the $t\bar{t}$ production signal diagrams of Figs. 1a, 1b, 2a, 2b and in the non double resonance diagrams of Figs. 1c, 1d and 2c.

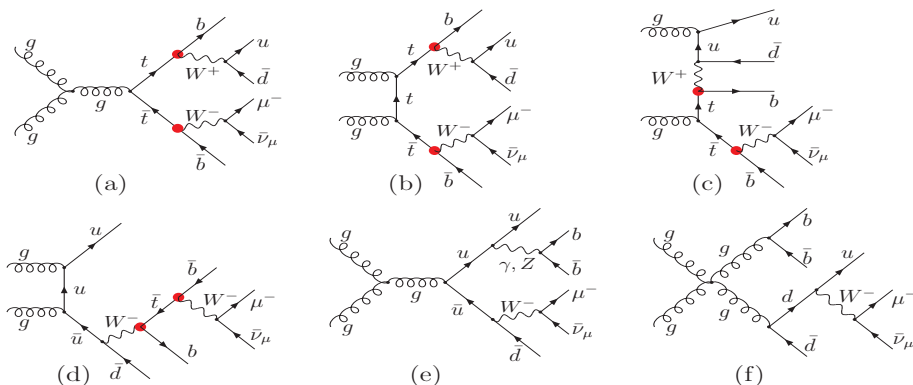


Figure 1: Examples of the leading order Feynman diagrams of process (4). Blobs indicate the Wtb coupling.

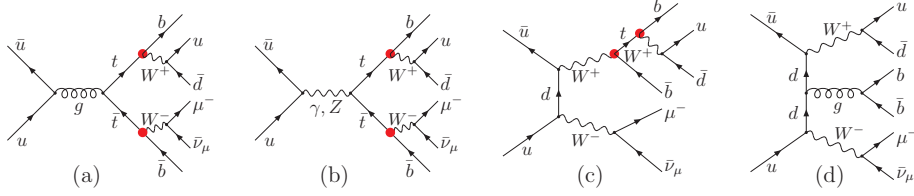


Figure 2: Examples of the leading order Feynman diagrams of process (5). Blobs indicate the Wtb coupling.

The effective Lagrangian of the Wtb interaction containing operators of dimension up to five considered in the present work has the following form [2]:

$$\begin{aligned}
L_{Wtb} = & \frac{g}{\sqrt{2}} V_{tb} \left[W_{\mu}^{-} \bar{b} \gamma^{\mu} \left(f_1^L P_L + f_1^R P_R \right) t \right. \\
& \left. - \frac{1}{m_W} \partial_{\nu} W_{\mu}^{-} \bar{b} \sigma^{\mu\nu} \left(f_2^L P_L + f_2^R P_R \right) t \right] \\
& + \frac{g}{\sqrt{2}} V_{tb}^* \left[W_{\mu}^{+} \bar{t} \gamma^{\mu} \left(\bar{f}_1^L P_L + \bar{f}_1^R P_R \right) b \right. \\
& \left. - \frac{1}{m_W} \partial_{\nu} W_{\mu}^{+} \bar{t} \sigma^{\mu\nu} \left(\bar{f}_2^L P_L + \bar{f}_2^R P_R \right) b \right], \quad (7)
\end{aligned}$$

where form factors f_i^L , f_i^R , \bar{f}_i^L and \bar{f}_i^R , $i = 1, 2$ can be complex in general and the remaining notation is obvious. See [7] for details and the corresponding Feynman rules. The lowest order SM Lagrangian of Wtb interaction is reproduced for $f_1^L = \bar{f}_1^L = 1$ and all the other form factors equal 0. CP conservation leads to the following relationships between the form factors of (7):

$$\bar{f}_1^{R*} = f_1^R, \quad \bar{f}_1^{L*} = f_1^L, \quad \bar{f}_2^{R*} = f_2^L, \quad \bar{f}_2^{L*} = f_2^R. \quad (8)$$

First direct limits on the form factors of (7) were obtained by the CDF Collaboration by investigating two form factors at a time while assuming the other two at their SM values [14]. The limits have been improved recently by the D0 Collaboration [15] and they read:

$$\left| V_{tb} f_1^R \right|^2 < 0.93, \quad \left| V_{tb} f_2^R \right|^2 < 0.13, \quad \left| V_{tb} f_2^L \right|^2 < 0.06. \quad (9)$$

More stringent are one-dimensional limits at 95% C.L. [15]:

$$\left| V_{tb} f_1^R \right|^2 < 0.50, \quad \left| V_{tb} f_2^R \right|^2 < 0.11, \quad \left| V_{tb} f_2^L \right|^2 < 0.05. \quad (10)$$

Limits derived from ATLAS [16] and CMS [17] measurements of W -boson helicity fractions using a program TOPFIT [18] with one non-zero coupling at a time and $V_{tb} = 1$ read:

$$\text{Re}f_1^R \in [-0.20, 0.23], \quad \text{Re}f_2^R \in [-0.08, 0.04], \quad \text{Re}f_2^L \in [-0.14, 0.11]. \quad (11)$$

Limits (11) are weaker if two couplings are varied at a time [17]. Amazingly enough, the right-handed vector form factor f_1^R is least constraint in (9)–(11), but if CP is conserved then it is indirectly constrained from the CLEO data on $b \rightarrow s\gamma$ [19] and from other rare B decays [20].

3 Results

Lagrangian (7) was implemented into `carlomat` [11], a general purpose program for the Monte Carlo (MC) computation of lowest order cross sections. A new version of the program [12] was already used to make predictions for the FBA in top quark production at the Tevatron [7]. In this section, a sample of results is presented that illustrate an influence of the tensor form factors of Lagrangian (7) on the distributions of the secondary μ^- in top quark pair production at the pp collisions at the LHC energies through reaction (3). As in [7], we put $V_{tb} = 1$ and assume form factors f_i^L , f_i^R , \bar{f}_i^L and \bar{f}_i^R , $i = 1, 2$, of Lagrangian (7) to be real. Moreover, the vector form factors are fixed at their SM values of $f_1^L = \bar{f}_1^L = 1$, $f_1^R = \bar{f}_1^R = 0$ and only the tensor form factors $f_2^{L,R}$, $\bar{f}_2^{L,R}$ are changed by assigning them two values: 0 or 0.2 in different, CP-even or CP-odd, combinations. A value of 0.2 that exceeds limits (9)–(11) is chosen just for the sake of illustration of the anomalous coupling effects that for smaller values of the form factors would have been hardly visible in the plots. However, an interested user can easily obtain predictions for any other choice of the form factors with the publicly available program [12].

The physical input parameters that are used in the computation are the same as in [7]. In order to avoid on-shell poles the following complex mass parameters:

$$m_b^2 \rightarrow M_b^2 = m_b^2 - im_b\Gamma_b, \quad b = Z, W, h, \quad m_t \rightarrow M_t = \sqrt{m_t^2 - im_t\Gamma_t} \quad (12)$$

are used instead of masses in propagators of unstable particles, both in the s - and t -channel. The particle widths in (12) are assumed to be constant

and the square root with positive real part is chosen, see [11] for details. The computation is performed in the complex mass scheme, where the electroweak (EW) couplings are parametrized in terms the complex EW mixing parameter $\sin^2 \theta_W = 1 - M_W^2/M_Z^2$ which preserves the lowest order Ward identities [21] and minimizes the unitarity violation effects at high energies.

The width of the top quark has substantial influence on the cross section of reaction (3). Therefore, it is calculated in the leading order for every specific choice of the form factors with effective Lagrangian (7) that, due to the fact that branching fractions of the decays $t \rightarrow bW^+$ and $\bar{t} \rightarrow \bar{b}W^-$ are close to 1, practically determines it. It should be stressed that for CP-odd choices of the form factors the widths Γ_t of t and $\Gamma_{\bar{t}}$ of \bar{t} differ from each other. Thus, the both widths are calculated and the following rule is applied to put the width in the s -channel top quark propagator: Γ_t is used if the propagator goes into bW^+ and $\Gamma_{\bar{t}}$ is used if the propagator goes into $\bar{b}W^-$. The rule does not work for the propagators in t -channel, but the actual value of the top quark width does not play much of a role there. If the prescription is applied then the $t\bar{t}$ production signal contribution to the cross section of (3) in the NWA takes the following form

$$\begin{aligned} \sigma(pp \rightarrow t^*\bar{t}^* \rightarrow bud\bar{b}\mu^-\bar{\nu}_\mu) \Big|_{\text{NWA}} \\ \approx \sigma(pp \rightarrow t\bar{t}) \frac{\Gamma_{t \rightarrow bW^+}}{\Gamma_t} \frac{\Gamma_{W^+ \rightarrow u\bar{d}}}{\Gamma_W} \frac{\Gamma_{\bar{t} \rightarrow \bar{b}W^-}}{\Gamma_{\bar{t}}} \frac{\Gamma_{W^- \rightarrow \mu^-\bar{\nu}_\mu}}{\Gamma_W} \\ \approx \sigma(pp \rightarrow t\bar{t}) \frac{\Gamma_{W^+ \rightarrow u\bar{d}}}{\Gamma_W} \frac{\Gamma_{W^- \rightarrow \mu^-\bar{\nu}_\mu}}{\Gamma_W} \end{aligned}$$

and unitarity is preserved. The unitarity argument can be also used to justify the prescription for the s -channel top quark propagator in the off resonance background Feynman diagrams which, as will be illustrated later, contribute very little to the cross section. However, a field theoretical justification of the effective prescription proposed would actually require calculation of higher order corrections to partonic processes (4)–(6) with nonrenormalizable Lagrangian (7). This formidable and delicate task is beyond the scope of this work.

The cross section of reaction (3) is calculated by folding CTEQ6L parton distribution functions (PDFs) [22] with the cross sections of underlying hard scattering processes (4), (5) and (6), with the cross sections of the quark-antiquark annihilation processes being symmetrized with respect to the interchange of the initial state quark and antiquark. The factoriza-

tion scale is assumed to be equal $Q = \sqrt{m_t^2 + \sum_j p_{Tj}^2}$. The $t\bar{t}$ production events are identified with the following acceptance cuts on the transverse momenta p_T , pseudorapidities η , missing transverse energy \cancel{E}^T and separation $\Delta R_{ik} = \sqrt{(\eta_i - \eta_k)^2 + (\varphi_i - \varphi_k)^2}$ in the pseudorapidity–azimuthal angle (φ) plane between the objects i and k :

$$p_{Tl} > 30 \text{ GeV}/c, \quad p_{Tj} > 30 \text{ GeV}/c, \quad |\eta_l| < 2.1, \quad |\eta_j| < 2.4,$$

$$\cancel{E}^T > 20 \text{ GeV}, \quad \Delta R_{lj,jj} > 0.4. \quad (13)$$

The subscripts l and j in (13) stand for *lepton* and *jet*, a direction of the latter is identified with the direction of the corresponding quark. Cuts (13) are rather restrictive which means that only slightly more than 1% of the MC events generated by `carlomat` pass them.

Effects of the anomalous Wtb coupling must be considered relative to the corresponding SM result. Therefore, in Figs. 3–6 the differential cross sections of (3) calculated with different choices of the tensor form factors of Lagrangian (7) and the vector form factors set to their SM values, i.e. $f_1^L = \bar{f}_1^L = 1$ and $f_1^R = \bar{f}_1^R = 0$, are each time plotted together with the corresponding SM cross section. The actual values of the tensor form factors used are always specified in a plot. The absolute size of the cross sections should be treated with great care, as it to large degree depends on the choice of PDFs or factorization scale. To diminish the dependence on the latter higher order QCD corrections should be taken into account. It should be also realized that the form factors get contributions from the EW loop corrections that, however, should be much smaller than the value of 0.2 used in the plots. The relative size of the modification is on the other hand independent of the choice of PDFs which has been checked explicitly by repeating the calculations with MSTW PDFs [23].

Figs. 3–6 show the results for a few distributions of the final state μ^- of reaction (3) at two different pp collision energies of 8 TeV and 14 TeV. In each of the figures, the SM cross section is plotted with grey boxes and the cross sections in the presence of different CP-even (two upper rows) and CP-odd (two lower rows) choices of the tensor form factors of Lagrangian (7) are plotted with solid lines. The transverse momentum and rapidity distributions of the μ^- are shown in Figs. 3 and 4. The distributions in $\cos\theta_{lb}$, where θ_{lb} is the angle between the momentum of μ^- in the pp centre of mass frame and the beam, are plotted in Fig. 5. Finally, the distributions in $\cos\theta^*$, where

θ^* is the angle between the momentum of μ^- and the reversed momentum of the b -quark, both boosted to the rest frame of the W -boson, are plotted in Fig. 6. Distributions in $\cos\theta^*$ are usually used in order to determine the helicity fractions of the W -boson produced in top quark decays, see, e.g., [16], [17].

Changes in the distributions are rather moderate, at most of the order of several per cent, both for the CP-even and CP-odd combinations of the tensor form factors. This observation can be regarded as another example of the decoupling theorem of [4] that was originally proven in the NWA, but now seems to work also for the off shell top quark pair production and decay in proton-proton collisions at the LHC energies. Although all the cross sections increase by about a factor 4 if the energy of pp collisions is increased from $\sqrt{s} = 8$ TeV to $\sqrt{s} = 14$ TeV, the relative changes caused by the tensor form factors are fairly independent of the pp collision energy, as can be seen by comparing plots on the left- and right-hand sides of Figs. 3–6. Let us note that shapes of the distributions remain practically unchanged by the non zero form factors, both in the CP-even and CP-odd case, except for the distribution in $\cos\theta^*$ of Fig. 6.

The distributions of μ^- of reaction (3) at $\sqrt{s} = 14$ TeV in the same variables as in Figs. 3–6 computed with the full set of leading order Feynman diagrams, plotted with the shaded boxes, and with the $t\bar{t}$ production signal diagrams, plotted with the dashed lines, are compared in Fig. 7. The comparison demonstrates very little effect of the off resonance background contributions in the presence of acceptance cuts (13). The results for other combinations of the tensor form factors, which are not shown, look very similarly.

4 Summary

A new version of `carlomat` [12], a general purpose program for the MC computation of lowest order cross sections, has been used to compute the transverse momentum, rapidity and two angular distributions of the final state μ^- of reaction (3) in the presence of the anomalous Wtb coupling with operators of dimension up to five. The considered CP-even and CP-odd combinations of the tensor form factors have rather small effect on the distributions which actually could be expected, as the top quarks are produced unpolarized. At the same time, the shapes of the presented distributions re-

main practically unchanged, except for the distribution in $\cos\theta^*$, where θ^* is the angle between the momentum of μ^- and the reversed momentum of the b -quark, both boosted to the rest frame of W -boson. It is just the change in shape of the $\cos\theta^*$ distribution that potentially gives the best prospects for improving limits on the tensor form factors in future measurements at the LHC.

It has been also shown that the off resonance background contributions have rather little impact on the distributions independently of whether the anomalous tensor form factors are present or not.

Acknowledgements: This project was supported in part with financial resources of the Polish National Science Centre (NCN) under grant decision number DEC-2011/03/B/ST6/01615 and by the Research Executive Agency (REA) of the European Union under the Grant Agreement number PITN-GA-2010-264564 (LHCPhenoNet).

References

- [1] M. Jezabek, J.H. Kühn, Nucl.Phys. **B320**, 20 (1989).
- [2] G.L. Kane, G.A. Ladinsky, C.-P. Yuan, Phys. Rev. **D45** (1992) 124.
- [3] B. Grzadkowski, Z. Hioki, Phys. Lett. **B476** (2000) 87, hep-ph/9911505; E. Boos, M. Dubinin, M. Sachwitz, H.J. Schreiber, Eur. Phys. J. **C16** (2002) 471.
- [4] B. Grzadkowski, Z. Hioki, Phys. Lett. **B476**, 87 (2000); Phys. Lett. **B529**, 82 (2002); Phys. Lett. **B557**, 55 (2003); S.D. Rindani, Pramana **54**, 791 (2000), hep-ph/0002006.
- [5] K. Ciećkiewicz, K. Kołodziej, Acta Phys. Pol. **B34** (2003) 5497.
- [6] K. Kołodziej, Phys. Lett. **B584** (2004) 89.
- [7] K. Kołodziej, Phys. Lett. **B710** (2012) 671.
- [8] CDF Collaboration, T. Aaltonen *et al.*, Phys. Rev. Lett. **101** (2008) 202001, arXiv:0806.2472; CDF Collaboration, T. Aaltonen *et al.*, arXiv:1101.0034.

- [9] D0 Collaboration, V.M. Abazov *et al.*, Phys. Rev. D **84**, (2011) 112005, arXiv:1107.4995.
- [10] L.G. Almeida, G.F. Sterman, W. Vogelsang, Phys. Rev. D **78** (2008) 014008;
 O. Antunano, J.H. Kühn, G. Rodrigo, Phys. Rev. D **77** (2008) 014003;
 M. T. Bowen, S. D. Ellis, D. Rainwater, Phys. Rev. D **73** (2006) 014008;
 S. Frixione, B.R. Webber, JHEP **06** (2002) 029;
 S. Frixione, *et al.*, JHEP **08** (2003) 007;
 V. Ahrens, A. Ferroglia, M. Neubert, B.D. Pecjak, L.L. Yang, arXiv:1106.6051;
 N. Kidonakis, arXiv:1105.5167;
 W. Hollik, D. Pagani, arXiv:1107.2606;
 J.H. Kühn, G. Rodrigo, arXiv:1109.6830.
- [11] K. Kołodziej, Comput. Phys. Commun. **180** (2009) 1671.
- [12] K. Kołodziej, Acta Phys. Polon. **B42** (2011) 2477;
 K. Kołodziej, arXiv:1305.5096. Program available from:
<http://kk.us.edu.pl/>.
- [13] K. Kołodziej, Phys. Lett. **B584** (2004) 89.
- [14] CDF Collaboration, T. Aaltonen *et al.*, Phys. Rev. Lett. **102** (2009) 092002.
- [15] D0 Collaboration, V.M. Abazov *et al.* Phys. Lett. **B708** (2012) 21.
- [16] ATLAS Collaboration, G. Aad *et al.*, arXiv:1205.2484.
- [17] CMS Collaboration, CMS-PAS-TOP-11-020 (2012).
- [18] J.A. Aguilar-Saavedra, J. Carvalho, N.F. Castro, F. Veloso, A. Onofre, Eur. Phys. J. **C50** (2007) 519;
 J.A. Aguilar-Saavedra, J. Bernabeu, Nucl. Phys. **B840** (2010) 349.
- [19] CLEO Collaboration, M.S. Alam *et al.*, Phys. Rev. Lett. **74**, 2885 (1995);
 F. Larios, M.A. Perez and C.-P. Yuan Phys. Lett **B457**, (1999) 334;
 G. Burdman, M.C. Gonzales-Garcia, S.F. Novaes, Phys. Rev. **D61** (2000) 114016;
 B. Grzadkowski, M. Misiak, Phys. Rev. **D78** (2008) 077501;

- J. P. Lee and K. Y. Lee, Phys. Rev. **D 78** (2008) 056004, and references therein.
- [20] J. Drobnak, S. Fajfer, J.F. Kamenik, arXiv:1109.2357;
A. Crivellin, L. Mercolli, arXiv:1106.5499.
- [21] A. Denner, S. Dittmaier, M. Roth, D. Wackerroth, Nucl. Phys. B560 (1999) 33 and Comput. Phys. Commun. 153 (2003) 462.
- [22] J. Pumplin et al., JHEP **07** (2002) 012.
- [23] A.D. Martin, W.J. Stirling, R. S. Thorne, G. Watt, Eur. Phys. J. **C63** (2009) 189-285.

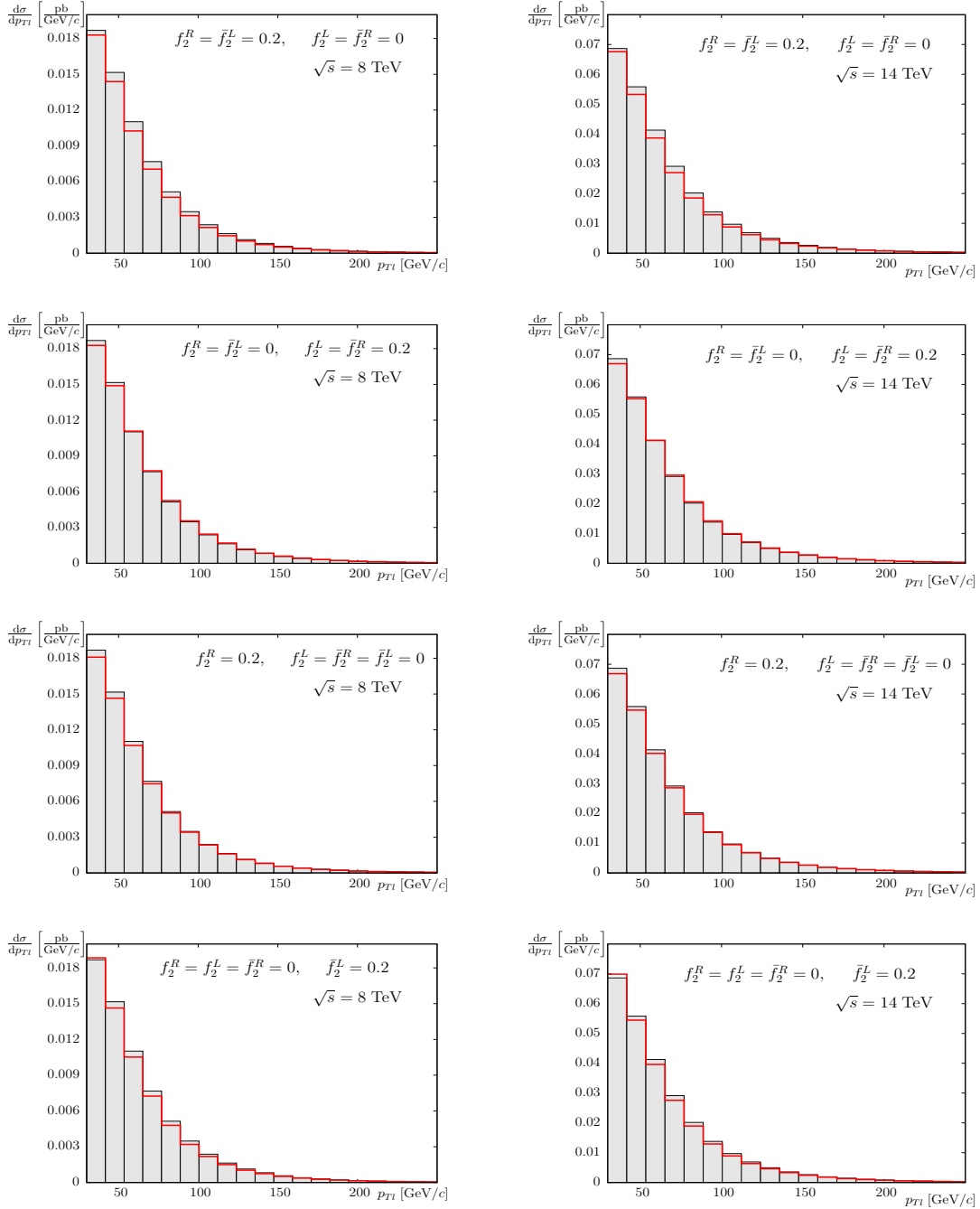


Figure 3: Distributions in p_T of the final state μ^- of reaction (3) in pp collisions at $\sqrt{s} = 8$ TeV (left) and $\sqrt{s} = 14$ TeV (right) for CP-even (two upper rows) and CP-odd (two lower rows) choices of the tensor form factors of (7).

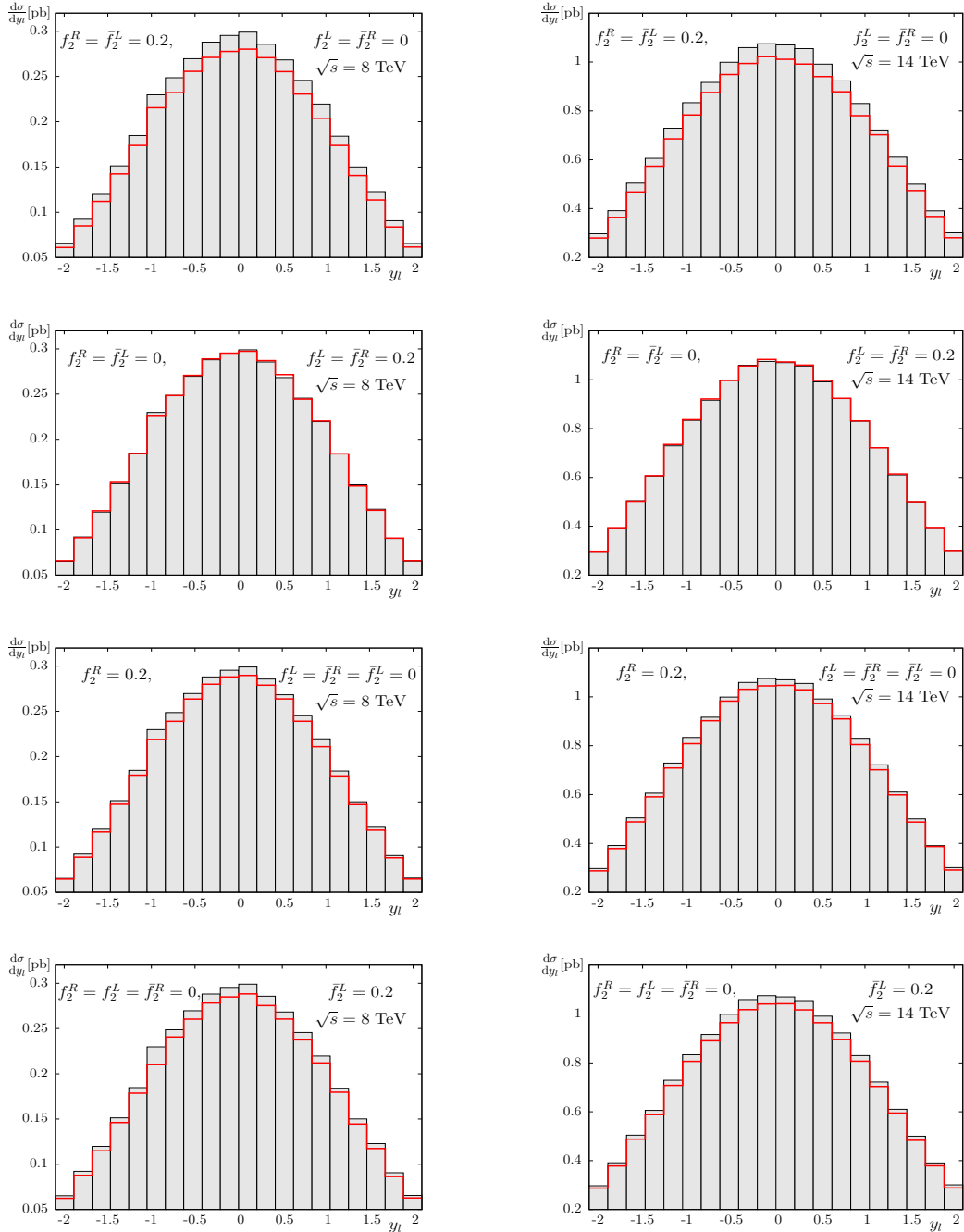


Figure 4: Distributions in rapidity of the final state μ^- of reaction (3) in pp collisions at $\sqrt{s} = 8$ TeV (left) and $\sqrt{s} = 14$ TeV (right) for CP-even (two upper rows) and CP-odd (two lower rows) choices of the tensor form factors of (7).

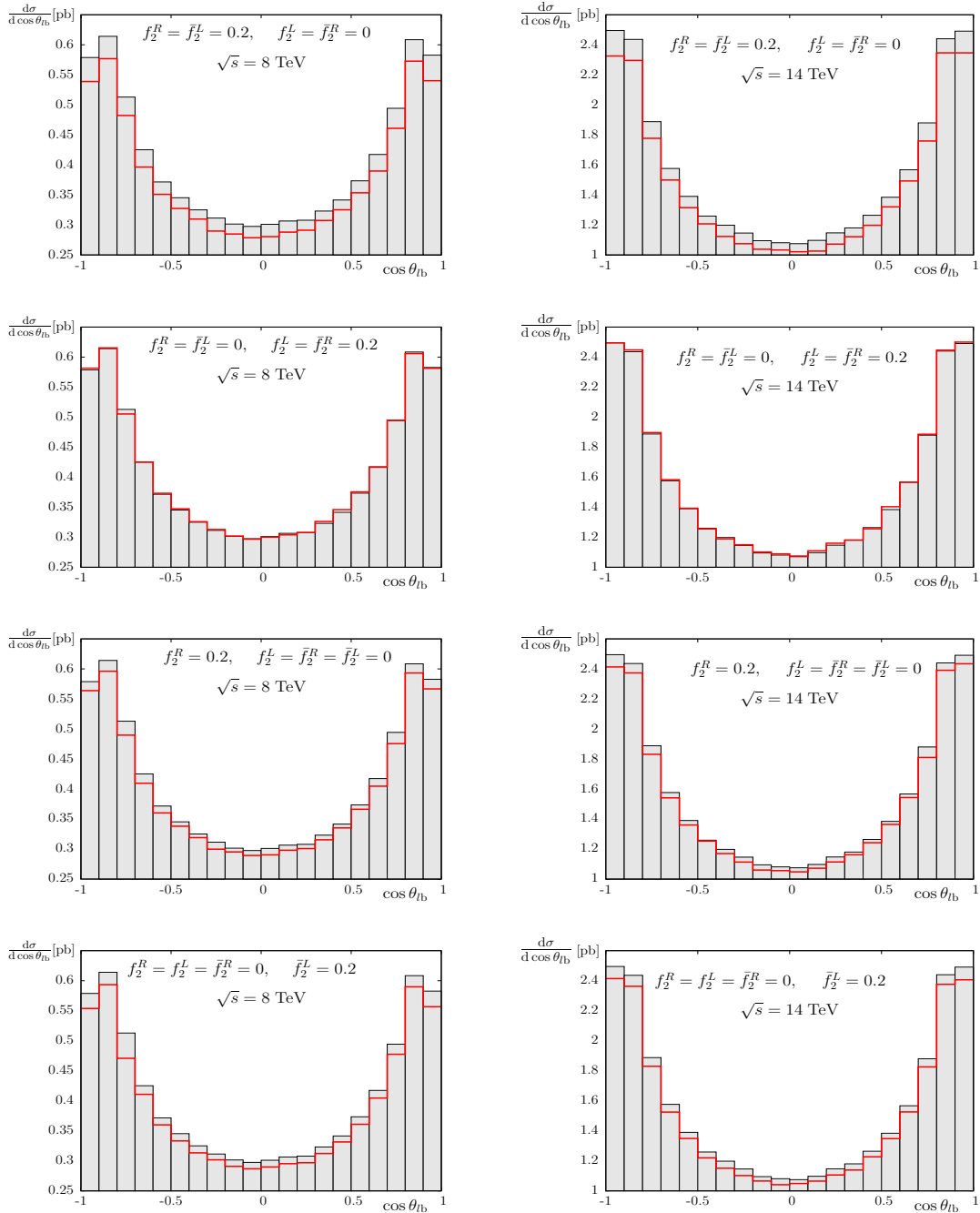


Figure 5: Distributions in $\cos \theta_{lb}$, with θ_{lb} being an angle between the momenta of the final state μ^- of reaction (3) and the beam, in pp collisions at $\sqrt{s} = 8$ TeV (left) and $\sqrt{s} = 14$ TeV (right) for CP-even (two upper rows) and CP-odd (two lower rows) choices of the tensor form factors of (7).

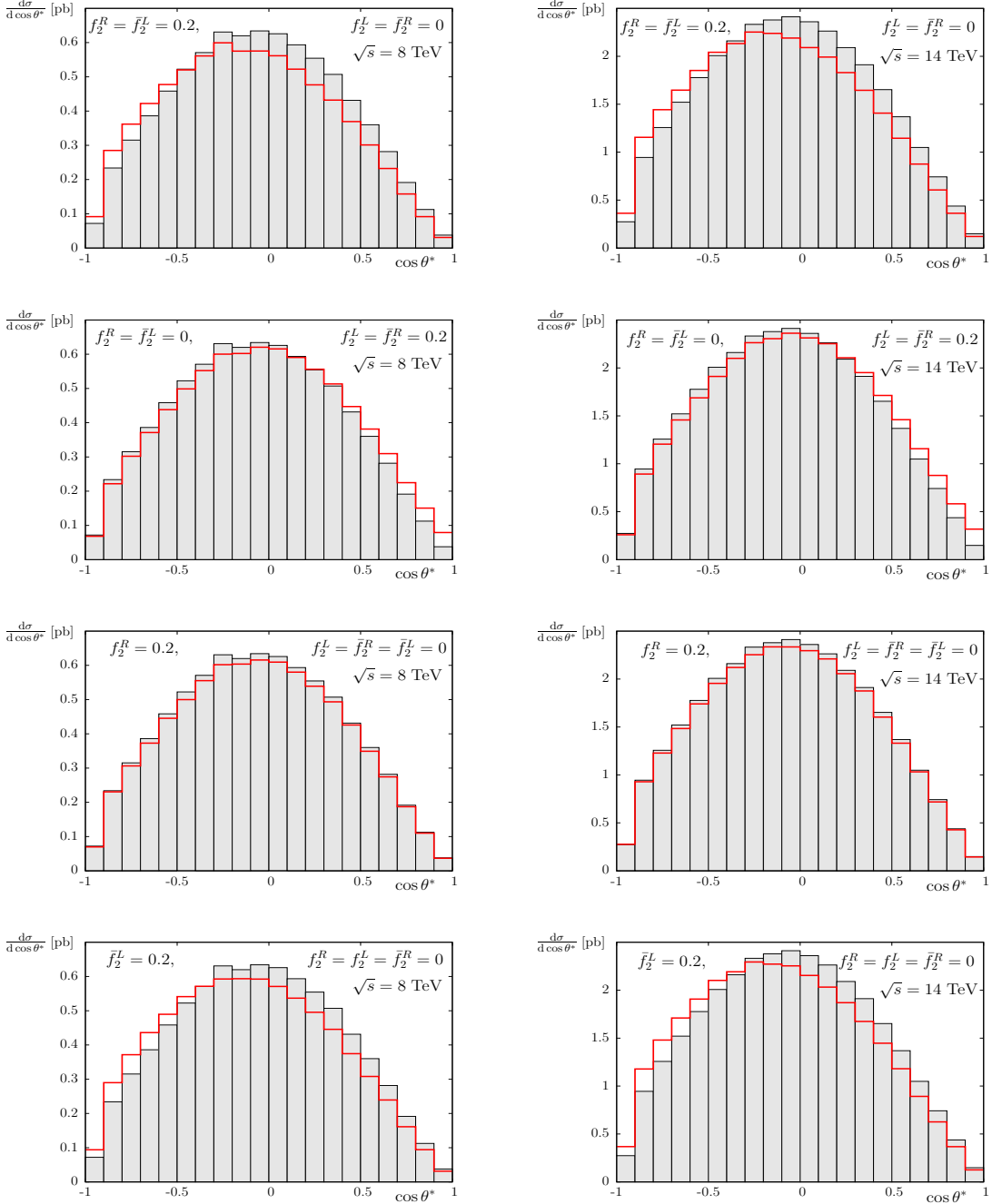


Figure 6: Distributions in $\cos\theta^*$, where θ^* is an angle between the momentum of μ^- and the reversed momentum of b -quark of (3), both boosted to the W -boson rest frame, in pp collisions at $\sqrt{s} = 8$ TeV (left) and $\sqrt{s} = 14$ TeV (right) for CP-even (two upper rows) and CP-odd (two lower rows) choices of the tensor form factors of (7).

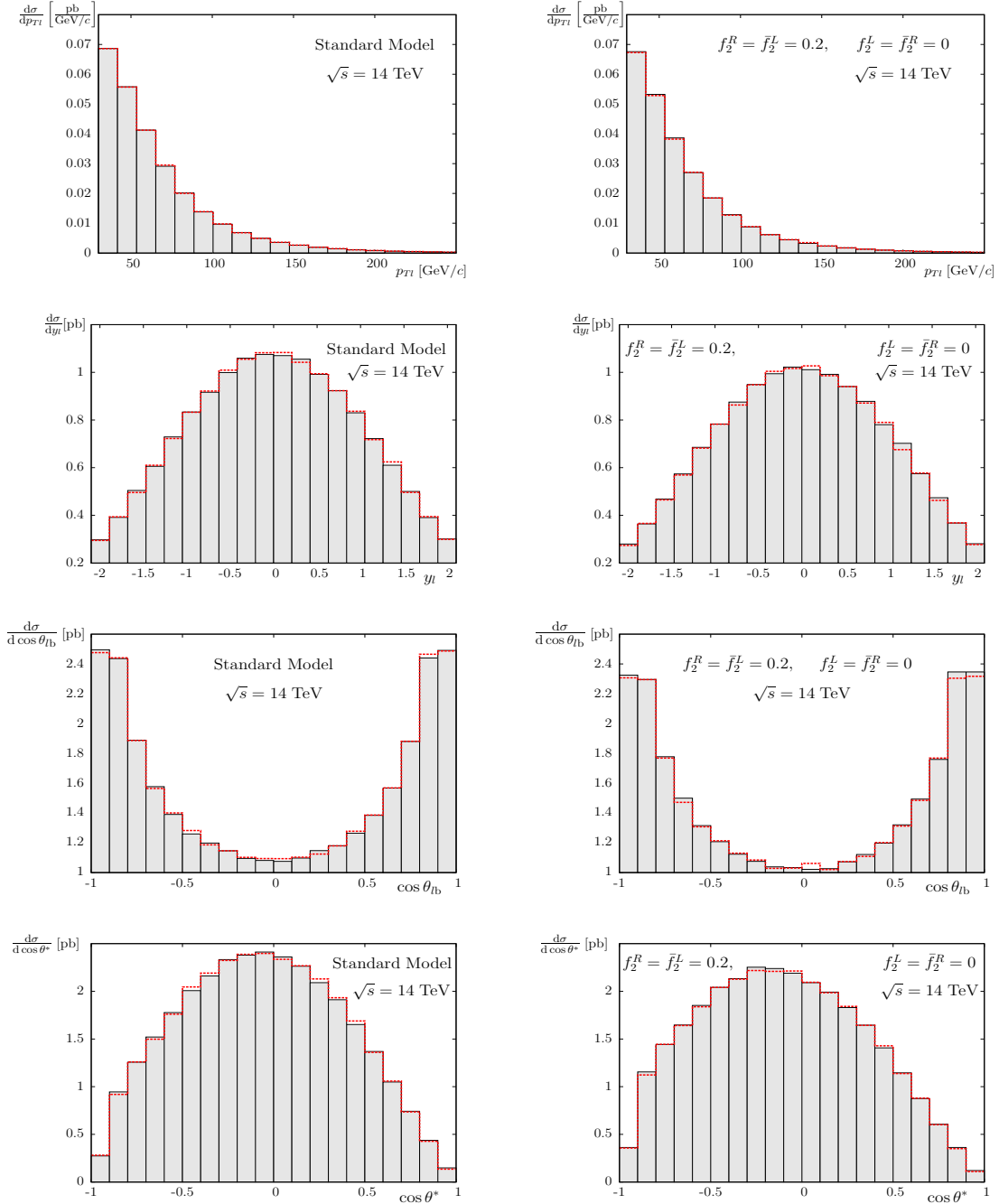


Figure 7: Distributions of μ^- of (3) at $\sqrt{s} = 14$ TeV in the same variables as in Figs. 3–6. The distributions computed with the full set of leading order Feynman diagrams are plotted with the shaded boxes and those computed with the $t\bar{t}$ production signal diagrams only are plotted with the dashed lines.